IEEE Access
Multidisciplinary | Rapid Review | Open Access Journal

Received 16 May 2024, accepted 17 June 2024, date of publication 26 June 2024, date of current version 3 July 2024.

Digital Object Identifier 10.1109/ACCESS.2024.3419724

RESEARCH ARTICLE

Model Predictive Control With Space Vector Modulation Based on a Voltage Angle for Driving Open-End Winding IPMSM

HYUNG-WOO LEE[1], (Student Member, IEEE), TAE-YONG YOON[2], (Student Member, IEEE), AND KYO-BEUM LEE[1], (Senior Member, IEEE)

[1]Department of Electrical and Computer Engineering, Ajou University, Suwon-si 16499, South Korea
[2]Department of Digital Appliances, Samsung Electronics, Suwon-si 16677, South Korea

Corresponding author: Kyo-Beum Lee (kyl@ajou.ac.kr)

This work was supported by the National Research Foundation of Korea (NRF) grant funded by the Ministry of Science and ICT (MSIT), the Korea Institute of Energy Technology Evaluation and Planning (KETEP), and the Ministry of Trade, Industry & Energy (MOTIE) of the Republic of Korea (No. RS-2024-00333208, No. 20225500000110).

ABSTRACT This paper proposes a model predictive control with space vector modulation (MPC-SVM) method that is based on using a voltage angle to reduce ripple components in open-end winding interior permanent magnet synchronous motor (OEW-IPMSM). Conventional model predictive control (CMPC) provides fast transient states by applying an actual voltage vector each switching period. However, due to the limited magnitude of voltage vectors, the CMPC causes large torque ripple and low current quality. The MPC-SVM method proposed herein generates virtual voltage vectors based on the voltage angle and surrounding area. Virtual voltage vectors provide various magnitudes and positions except for areas that are not in use. The optimal reference voltage vector is derived as the result of the cost function operation applied through the space vector modulation (SVM) method, and it improves the steady-state compared to the CMPC. Therefore, torque ripple is reduced and current quality is improved by using fewer virtual voltage vectors, and this results in superior steady-state characteristics. The validity of the proposed MPC-SVM method based on the voltage angle for driving OEW-IPMSM is affirmed through simulation and experimental results in comparison to the CMPC.

INDEX TERMS Open-end winding (OEW), interior permanent magnet synchronous motor (PMSM), model predictive control (MPC), space vector modulation (SVM), voltage angle, torque ripple, calculation burden.

I. INTRODUCTION

Interior permanent magnet synchronous motor (IPMSM) has been actively used in various industries through the specific means of high torque, efficiency, and power density [1], [2]. To drive an IPMSM, various voltage source inverters are used to apply the appropriate voltage at each phase of stators. In recent years, a dual inverter has come to be widely used, as it offers a higher voltage usage ratio than a single inverter. A DC-DC converter is typically used at the DC-link voltage stage to boost the voltage of an inverter, but this causes the system to experience an increase in weight or volume as well as higher costs [3], [4], [5]. Therefore, applying the dual inverter improves upon disadvantages of the DC-DC converter and reduces the complexity of the system. To drive an IPMSM fed by a dual inverter, it is necessary to use an open-end winding interior permanent magnet synchronous motor (OEW-IPMSM), with the stator windings having an open connection structure [6], [7].

Among the available strategies for controlling the torque of OEW-IPMSM, PI controllers are widely used due to their high performance in steady-state responses. Meanwhile, various methods such as direct torque control (DTC), and model predictive control (MPC) are also being applied as

The associate editor coordinating the review of this manuscript and approving it for publication was Feifei Bu.

alternatives to improve transient state responses [8], [9]. In the voltage source inverter, MPC selects the optimal voltage vector that has the smallest error between the reference and estimated value through the model equation of loads. MPC provides fast responsiveness with a simple algorithmic structure by directly applying the voltage vector without requiring additional controllers. To drive the IPMSM using MPC, the stator flux, torque, or current for the next control period are predicted through the discrete current model of the motor. The optimal voltage vector is applied by utilizing a cost function that stores the error between the reference and predicted values [10], [11].

The conventional model predictive control (CMPC) method applies only one voltage vector that has real switching states of the inverter within the control period [12], [13]. Therefore, a control parameter promptly follows the reference, thus providing a fast transient response. However, for the same reason, the switching frequency is not constant, which causes high ripple components in the steady-state. Applying the CMPC method to IPMSM results in high torque ripple in the steady-state and deteriorates the currents quality. It also leads to significant mechanical noise and vibration [14], [15].

The model predictive control with space vector modulation (MPC-SVM) method was proposed to improve upon the steady-state characteristics of the CMPC method. The MPC-SVM method generates not only voltage vectors that have real switching states, but also virtual voltage vectors that have various magnitudes and phases. A collection of virtual voltage vectors enhances the steady-state by selecting the voltage vector that closely follows the reference value, and it maintains a constant switching frequency through space vector modulation [16], [17]. However, virtual voltage vectors impose a calculation burden on the microprocessor due to the increased number of cost function calculations. Therefore, deadbeat methods have been actively researched in attempts to limit or select the specific region where virtual voltage vectors are generated. By using an appropriate number of virtual voltage vectors as candidates through a specific region, control performance is maintained while the calculation burden is minimized [18], [19].

This paper proposes the MPC-SVM method based on a voltage angle to improve the steady-state characteristics for driving OEW-IPMSM. The proposed method includes the deadbeat strategy, which generates virtual voltage vectors in the specified positions to select the optimal voltage vector and reduce the number of calculations in the cost function. In addition, the compensation method is applied to improve the timing error of voltage application as well as the rising or falling time errors of switching devices in the actual system. The proposed method improves the quality of current and torque more efficiently compared to several existing MPC-SVM methods by constraining generation region of the virtual voltage vector. This offers advantages in terms of computational burden by achieving the required quality with fewer virtual voltage vectors. The proposed method is implemented by the dual inverter utilizing isolated voltage sources. The effectiveness of the proposed MPC-SVM based on the voltage angle method is demonstrated through simulation and experimental results, and through comparison with the CMPC method.

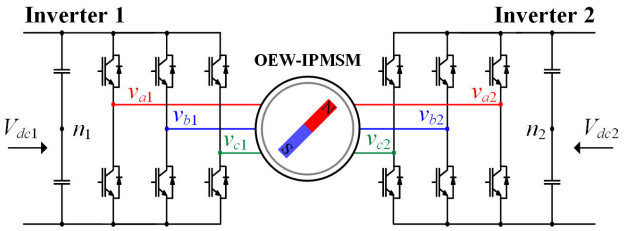

FIGURE 1. System circuit diagram for driving the OEW-IPMSM.

II. MATHEMATICAL MODEL OF OEW-IPMSM FED BY THE DUAL INVERTER

A. VOLTAGE MODEL EQUATION OF THE DUAL INVERTER

Among the various types of voltage source inverters, the dual inverter is used to drive open-end winding motors wherein both ends of the stator winding are open. Fig. 1 shows the system circuit diagram for driving the OEW-IPMSM. Since independent voltage sources are used, the DC-links of each inverter is separated. In the dual inverter with isolated voltage sources, the voltages of each inverter are expressed the same as they are in a single 2-level inverter, as follows

$$\begin{aligned} v_{an(z)} &= V_{dc(z)}\left(S_{a(z)} - 0.5\right) \\ v_{bn(z)} &= V_{dc(z)}\left(S_{b(z)} - 0.5\right) \\ v_{cn(z)} &= V_{dc(z)}\left(S_{c(z)} - 0.5\right) \\ v_{a(z)} &= V_{dc(z)}\left(2S_{a(z)} - S_{b(z)} - S_{c(z)}\right)/3 \\ v_{b(z)} &= V_{dc(z)}\left(2S_{b(z)} - S_{c(z)} - S_{a(z)}\right)/3 \\ v_{c(z)} &= V_{dc(z)}\left(2S_{c(z)} - S_{a(z)} - S_{b(z)}\right)/3 \end{aligned} \tag{1}$$

where z, $S_{abc(z)}$, $v_{abcn(z)}$, $v_{abc(z)}$, and $V_{dc(z)}$ represent inverter 1 or inverter 2, switching states, pole voltages, phase voltages, and DC-link voltages, respectively. Based on the structure of the dual inverter, inverter 1 and inverter 2 have a 180° phase difference, and the pole voltages and phase voltages of the dual inverter are expressed as follows

$$\begin{aligned} v_{an} &= v_{an1} - v_{an2} \quad v_a = v_{a1} - v_{a2} \\ v_{bn} &= v_{an1} - v_{an2} \quad v_b = v_{b1} - v_{b2} \\ v_{cn} &= v_{an1} - v_{an2} \quad v_c = v_{c1} - v_{c2} \end{aligned} \tag{2}$$

where v_{abcn} and v_{abc} respectively represent the pole voltages and phase voltages of the dual inverter, which generates and outputs a greater variety of voltage compositions compared to the 2-level single inverter. In addition, the output is doubled when the magnitudes of the DC-link voltages of inverters are independent and identical.

B. VOLTAGE MODEL EQUATION OF THE OEW-IPMSM

OEW-IPMSM has the same voltage equations as a general IPMSM in the d-q axes rotor reference frame due to its structure in which only the winding ends are open, and it is represented as

$$\begin{aligned} v_{de} &= R_s i_{de} + \frac{d\lambda_{de}}{dt} - \omega_e \lambda_{qe} \\ v_{qe} &= R_s i_{qe} + \frac{d\lambda_{qe}}{dt} + \omega_e \lambda_{de} \end{aligned} \tag{3}$$

where v_{dqe}, i_{dqe}, λ_{dqe}, R_s, and ω_e represent stator voltages, currents, fluxes, resistance, and electrical angular frequency, respectively. The electrical torque and stator flux of the OEW-IPMSM can also be represented in the d-q axes rotor reference frame and expressed as follows

$$\begin{aligned} T_e &= \frac{3}{2} P_n \left[\phi_f i_{qe} + \left(L_d - L_q \right) i_{de} i_{qe} \right] \\ \lambda_{de} &= L_d i_{de} + \phi_f \\ \lambda_{qe} &= L_q i_{qe} \end{aligned} \tag{4}$$

where ϕ_f, T_e, P_n, and L_{dq} represent permanent magnet flux, electrical torque, half the number of poles, and d-q axes inductances. The difference in inductances along the d-q axes, represented by $L_d - L_q$, arising from the permanent magnet arrangement structure of the OEW-IPMSM not only generates electrical torque due to the permanent magnets, but it also introduces a reluctance component. The voltage model equation is also expressed by substituting (4) into (3) as follows

$$\begin{aligned} v_{de} &= R_s i_{de} + L_d \frac{di_{de}}{dt} - \omega_e L_q i_{qe} \\ v_{qe} &= R_s i_{qe} + L_q \frac{di_{qe}}{dt} + \omega_e L_d i_{de} + \omega_e \phi_f \end{aligned} \tag{5}$$

Equation (5) is expressed in the differential form and used in MPC through transformation to the current model.

III. CONVENTIONAL MPC METHOD FOR DRIVING THE OEW-IPMSM

A. DISCRETE TIME MODEL OF THE OEW-IPMSM

MPC estimates the output value in the next control period from the candidates of input value from the model equation of loads. To predict the electrical torque and stator flux according to the control period, the stator voltage model equation represented by (5) needs to be transformed into a discrete time current model that can be expressed in terms of the sampling time. To transform the continuous time current model equation with respect to analog time (t) into a discrete time current model equation with respect to sampling time (T_{samp}), an approximation is applied to the derivative terms as follows

$$\frac{di_{dqe}}{dt} \cong \frac{i_{dqe}(k) - i_{dqe}(k-1)}{T_{samp}} \simeq \frac{i_{dqe}(k+1) - i_{dqe}(k)}{T_{samp}} \tag{6}$$

where k-1, k, and $k+1$ represent the previous, current, and next control period values, respectively. After applying the approximation, (5) can be expressed in terms of the stator current in the d-q axes rotor reference frame as follows

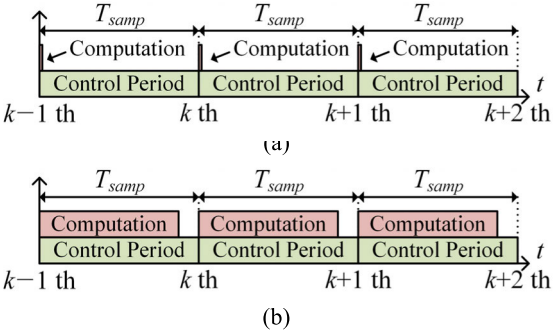

FIGURE 2. Comparison of computation time. (a) Simulation tools and (b) actual system.

$$\begin{aligned} i_{de}(k+1) &= \left(1 - R_s T_{samp}/L_d\right) i_{de}(k) \\ &\quad + \left(L_q T_{samp}/L_d\right) \omega_e i_{qe}(k) \\ &\quad + v_{de}(k+1)\, T_{samp}/L_d \\ i_{qe}(k+1) &= \left(1 - R_s T_{samp}/L_q\right) i_{qe}(k) \\ &\quad + \left(L_q T_{samp}/L_d\right) \omega_e i_{de}(k) \\ &\quad + \left(v_{qe}(k+1) - \phi_f \omega_e\right) T_{samp}/L_q \end{aligned} \tag{7}$$

However, in an actual system, it is necessary to include a delay compensation method for errors in signal transmission or the timing of switching signal application to power devices occurring in hardware. Fig. 2 shows the comparison of computation time between simulation tools and the actual system. in the simulation tools, the next switching states are computed immediately, and the voltage vector is applied. However, the actual system requires some computation time to calculate the next states, which causes one period delay in the MPC. Therefore, to estimate the actual current for the next cycle as the value for the $k+2$th cycle, it is necessary to estimate the current for the $k+1$th cycle from a previous applied voltage vector and use it as the current for the current cycle. As a result, equation (7) in the actual system is utilized by applying the delay compensation method as follows

$$\begin{aligned} i_{de}(k+2) &= \left(1 - R_s T_{samp}/L_d\right) i_{de}(k+1) \\ &\quad + \left(L_q T_{samp}/L_d\right) \omega_e i_{qe}(k+1) \\ &\quad + v_{de}(k+2)\, T_{samp}/L_d \\ i_{qe}(k+2) &= \left(1 - R_s T_{samp}/L_q\right) i_{qe}(k+1) \\ &\quad + \left(L_q T_{samp}/L_d\right) \omega_e i_{de}(k+1) \\ &\quad + \left(v_{qe}(k+2) - \phi_f \omega_e\right) T_{samp}/L_q \end{aligned} \tag{8}$$

Using equation (8), the continuous time stator flux in (4) can be derived as a discrete time model and shown as

$$\begin{aligned} \lambda_s(k+2) &= \sqrt{\lambda_{de}^2(k+2) + \lambda_{qe}^2(k+2)} \\ &= \sqrt{\left(L_d i_{de}(k+2) + \phi_f\right)^2 + \left(L_q i_{qe}(k+2)\right)^2} \end{aligned} \tag{9}$$

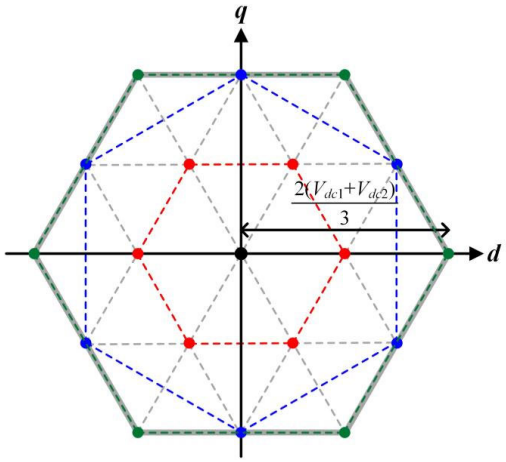

FIGURE 3. Voltage vector diagram of the dual inverter.

where λ_s represents the magnitude of stator flux. Using the same approach, the discrete time model for the electrical torque is as follows

$$T_e(k+2) = \frac{3}{2}P_n\left[\lambda_s(k+2)\, i_{qe}(k+2) + \left(L_d - L_q\right) i_{de}(k+2)\, i_{qe}(k+2)\right] \quad (10)$$

B. CANDIDATE VOLTAGE VECTORS AND COST FUNCTION

The CMPC method uses voltage vectors with actual switching states as candidate input voltages for the dual inverter to estimate the electrical torque and the stator flux in the next control period. Fig. 3 shows the voltage vector diagram of the dual inverter. When the DC-link voltages are identical and independent, 19 voltage vectors in total are used as candidate voltage vectors. In Fig. 3, each point represents the voltage vector of the dual inverter depicted in the d-q axes stationary reference frame. Depending on the switching states of each inverter, three magnitudes of effective vectors are synthesized along with a zero voltage vector. The generated voltage vectors are used as candidates for $v_{dqe}(k+2)$ in (8). Subsequently, the results of comparing the electrical torque and stator flux of the next control period with the reference, which are computed using the stored voltage vectors, are saved in the cost function (C), which as follows

$$C = F_\lambda\left|\lambda_s^* - \lambda_s(k+2)\right| + F_T\left|T_e^* - T_e(k+2)\right| \quad (11)$$

where F_λ, F_T, and * represent the weighting factor of stator flux, electrical torque, and the reference value, respectively. Weighting factors determine the necessary compensation for differences in magnitude when computing errors for two or more parameters, or they prioritize them from a control perspective. The candidate voltage vector that minimizes the cost function is selected as the reference voltage of the dual inverter, the dual inverter, and the switching state corresponding to reference voltage is applied during the next control period.

IV. PROPOSED MPC-SVM METHOD BASED ON A VOLTAGE ANGLE

A. VOLTAGE ANGLE ESTIMATION

To apply the proposed MPC-SVM method to drive the OEW-IPMSM, it is necessary to estimate the angle of voltage vector for the next control period. The voltage angle is estimated through the discrete time voltage model as follows

$$\begin{aligned}\hat{v}_{de} &= \left(R_s + L_d/T_{samp} - L_q/T_{samp}\right) i_{de}(k+1) \\ &\quad - L_q\omega_e i_{qe}(k+1) \\ \hat{v}_{qe} &= \left(R_s + L_q/T_{samp} - L_d/T_{samp}\right) i_{qe}(k+1) \\ &\quad + L_d\omega_e i_{de}(k+1) + \omega_e\phi_f \end{aligned} \quad (12)$$

where $\hat{v}_{dqe}$ represents the estimated voltage in the d-q axes rotor reference frame, which is derived from the addition of the voltage drop in stator winding, back-EMF, and mutual interference components. Equation (12) is transformed into the d-q axes rotor reference frame values, and the estimated voltage angle is expressed as

$$\theta_v = \tan^{-1}\left(\frac{\hat{v}_{qs}}{\hat{v}_{ds}}\right) \quad (13)$$

where θ_v and $\hat{v}_{dqs}$ represent the estimated voltage angle which is ultimately used in the proposed method and the estimated voltage in the d-q axes stationary reference frame, respectively.

B. VIRTUAL VOLTAGE VECTORS GENERATION

A number of candidate voltage vectors require a large amount of calculation on the microprocessor, thus leading to an increased calculation burden. Depending on the performance of the microprocessor used, it may be impossible to perform calculations within the control period. Therefore, for MPCs using the space vector modulation method, various deadbeat methods have been proposed or applied in attempts to exclude candidate voltage vectors from the calculation in regions where the reference value could not be followed. The proposed MPC-SVM method also applies the deadbeat method by only restricting the generation of virtual voltage vectors around the voltage angle. Fig. 4 shows an example of generating virtual voltage vectors in the proposed MPC-SVM method. The virtual voltage vector generation region is limited by the voltage angle and its surrounding two angles, and the number of virtual voltage vectors generated at each position is the same. Given the difference between the voltage angle and the surrounding angle (θ_d) and the number of vectors at each position (N), the number of virtual voltage vectors generated without applying the deadbeat method is determined as follows

$$G(N) = \left|\frac{360}{\theta_d}\right|(N-1) + 1 \quad (14)$$

where $G(N)$ represents the numerical equation of the number of candidate voltage vectors without the deadbeat method, where virtual voltage vectors are generated throughout the entire region. Applying the deadbeat method to enable the

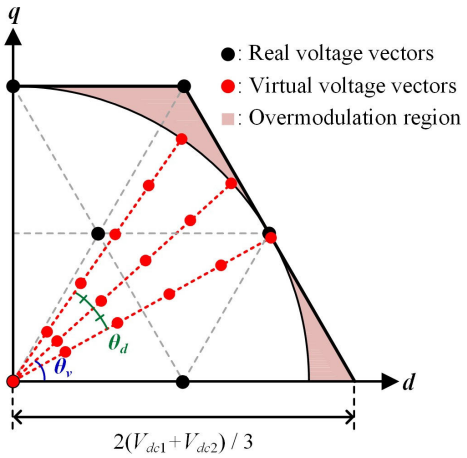

FIGURE 4. Example of generating virtual voltage vectors in the proposed MPC-SVM method.

generation of virtual voltage vectors from the voltage angle and its surrounding angles results in the following

$$G_{DB}(N) = 3\,(N-1) + 1 \tag{15}$$

where $G_{DB}(N)$ represents the numerical equation of the number of candidate voltage vectors when using the proposed deadbeat method. For instance, when θ_d is 10° and N is 5, before applying the deadbeat method, 145 calculations are required, but after applying the proposed deadbeat method, only 13 calculations are required. Compared to the CMPC method, which uses 19 actual voltage vectors, the proposed method that uses fewer virtual voltage vectors results in a reduced number of calculations, thus alleviating the calculation burden on the microprocessor. The proposed MPC-SVM method uses the discrete-time current model and cost function of the OEW-IPMSM in a manner identical to the CMPC method. Therefore, it is necessary to use a formula to derive the magnitudes of the virtual voltage vectors. When the coordinate number of virtual voltage vector is defined as x, the formula is as follows

$$x \in \frac{a}{N} \quad \{a = 1, 2, 3, \ldots, N\} \tag{16}$$

The magnitude of the virtual voltage vectors generated using the coordinate number is as follows

$$\begin{aligned} v_{ds(vir)} &= 0, \quad \frac{V_{dc1}+V_{dc2}}{\sqrt{3}} x \cos(\theta_v \pm \theta_{dev}) \\ v_{qs(vir)} &= 0, \quad \frac{V_{dc1}+V_{dc2}}{\sqrt{3}} x \sin(\theta_v \pm \theta_{dev}) \end{aligned} \tag{17}$$

where $v_{dqs(vir)}$ represents the magnitude of the virtual voltage vector. The zero voltage vector is only used once to avoid duplication.

C. SPACE VECTOR MODULATION AND DEAD TIME COMPENSATION

In voltage source inverters, dead time serves as a cause of nonlinearity due to errors between command voltage and output voltage. Despite recent advancements in switch device technology, dead time compensation must be considered for further enhancement of torque control performance in motor drive systems. In the proposed MPC-SVM method, the selected voltage vector is applied through the space vector modulation by two active voltage vectors and zero vectors. The various magnitudes and phases of the virtual voltage vectors lead to the production of stable electrical torque and improved current quality compared to the CMPC method. The selected reference voltage needs to be separated into a reference voltage for each inverter, as follows

$$v^*_{dqe(z)} = \frac{z_s \cdot V_{dc(z)}}{V_{dc1}+V_{dc2}} \cdot v^*_{dqe} \begin{cases} z_s = 1 & (z=1) \\ z_s = -1 & (z=2) \end{cases} \tag{18}$$

where v^*_{dqe}, and $v^*_{dqe}(z)$ represent the reference voltage and the reference voltage separated for each inverter, respectively. The separated reference voltages are transformed into three-phase reference voltages, and the switching states are determined through comparisons to carrier waves. However, in an actual system, switching devices include dead time to prevent shorts from the difference between the rising and falling times. Fig. 5 shows an example of the effect of dead time in reference voltage. Including dead time causes the magnitude of the output voltage to either decrease or increase, thus leading to errors between the estimated values and the actual output in the next control period. To compensate for errors caused by dead time, a dead time compensation method is required for three-phase reference voltages depending on the direction of the current, as follows

$$\begin{aligned} v_{dead(z)} = \frac{T_{dead}}{T_{samp}} \cdot V_{dc(z)} \begin{cases} \beta_{abc} = +1\,(i_{abc} > 0) \\ \beta_{abc} = -1\,(i_{abc} < 0) \end{cases} \\ \times \begin{cases} v^*_{abc1\_d} = v^*_{abc1} + \beta_{abc} v_{dead1} \\ v^*_{abc2\_d} = v^*_{abc2} + \beta_{abc} v_{dead2} \end{cases} \end{aligned} \tag{19}$$

where $v_{dead(z)}$, β_{abc}, i_{abc}, T_{dead}, $v^*_{abc(z)}$, and $v^*_{abc(z)\_d}$ respectively represent the compensated voltage, sign of the compensated voltage, abc-phase currents, settled dead time, reference voltages, and reference voltages after the dead time compensation method is applied [20]. Fig. 6 shows the control block diagram of the proposed MPC-SVM method for driving the OEW-IPMSM, which includes the overall processes of the proposed method.

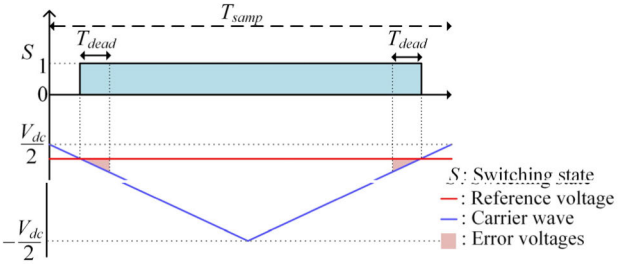

FIGURE 5. Example of the effect of dead time in reference voltage.

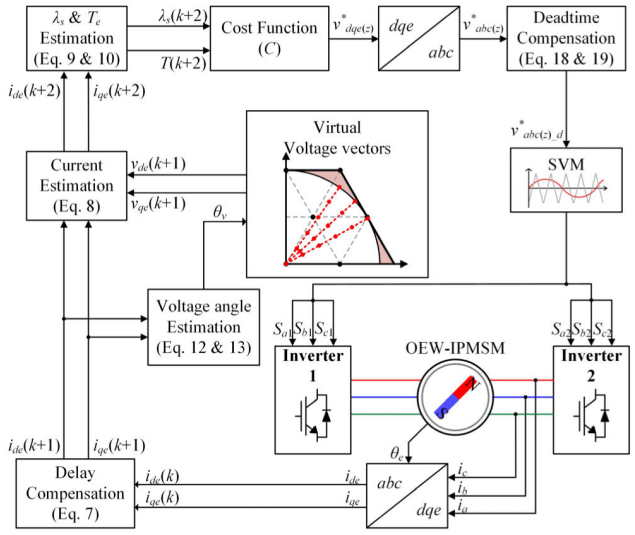

FIGURE 6. Control block diagram for the proposed MPC-SVM method for driving the OEW-IPMSM.

TABLE 1. Parameters of the OEW-IPMSM.

Parameters	Value	Unit
Rated power	2.2	[kW]
Rated speed	1750	[rpm]
Rated torque	12	[Nm]
Number of poles	12	
Stator resistance	0.213	[Ω]
d-axis inductance	1.6	[mH]
q-axis inductance	2.18	[mH]
Permanent magnet flux	0.113	[Wb]

In MPC method based on mathematical modeling of the system, variations in motor parameters degrade control performance. In the proposed MPC method as well, parameter variations reduce the accuracy of the modeling equations, thus deteriorating the estimation performance of the variables for next period. As an alternative to prevent the decrease in control performance caused by these parameter variations, the parameter table is commonly employed.

V. SIMULATION RESULTS

The proposed MPC-SVM based on a voltage angle method was demonstrated and compared to the CMPC method through PSIM simulation. Table 1 lists the parameters of the OEW-IPMSM whereas Table 2 lists the parameters of the simulation environments. The switching frequency and control period were set to 20 kHz and 50 μs. The CMPC method required 19 calculations for real voltage vectors. The dividing angle (θ_d) and the number of virtual voltage vectors per angle (N) were set to 10° and 5, respectively, so the number of virtual voltage vectors required in the proposed MPC-SVM method is 13, which leads to fewer calculations being required compared to the CMPC method. The DC-link

TABLE 2. Parameters of simulation environments.

Parameters	Value	Unit
DC-link voltage of inverter 1	75	[V]
DC-link voltage of inverter 2	75	[V]
Control period	50	[μs]
Switching frequency	20	[kHz]
Dividing angle (θ_d)	10	[degree]
Number of virtual voltage vectors per angle (N)	5	
Dead time	2	[μs]

voltage of both inverters was 75 V, which were independently applied. The initial values of each weighting factors were determined by normalizing them based on the rated value. Due to the normalization of weighting factors, errors in flux and torque are compared in the cost function at the same ratio. The ratio of normalized F_T and F_λ based on the rated values in Table 1 is 1:106, and the final ratio of the weight factors was determined through experimental adjustment based on the initial values.

Fig. 7(a) and 7(b) show the simulation results of torque control at 500 rpm in the CMPC method and the proposed MPC-SVM method. The reference electrical torque was changed from 2.4 Nm to 6 Nm. The transient times were 156 μs in the CMPC method and 166 μs in the proposed MPC-SVM method, and they were little changed or unchanged in the transient response. The total harmonic distortion (THD) of the current was improved from 21.31% to 2.53%.

Fig. 8(a) and 8(b) show the simulation results of torque control at 800 rpm in the CMPC method and the proposed MPC-SVM method. In the same manner as described for Fig. 7, the electrical torque was changed from 2.4 Nm to 6 Nm. The transient time in the CMPC method was 261 μs whereas that in the proposed method was 288 μs. The THD of the current was improved from 20.83% to 2.83%.

VI. EXPERIMENTAL RESULTS

The proposed MPC-SVM based on a voltage angle method was verified experimentally and compared to the CMPC method. Fig. 9 shows the experimental setup and the microprocessor (TMS320F28377S) used. The parameters of OEW-IPMSM and the experimental environments were identical to those in the simulations described in Table 1 and Table 2. Fig. 10 (a) and 10(b) show the experimental results of torque control at 500 rpm in the CMPC method and the proposed MPC-SVM method. The reference electrical torque was changed from 2.4 Nm to 6 Nm. The ripple components of stator flux and electrical torque were decreased in the proposed method. Compared to the reference value, the magnitude of average electrical torque ripple was decreased from 2.53 Nm to 0.76 Nm.

Fig. 11(a) and 11(b) show the experimental results of torque control at 800 rpm in the CMPC method and the

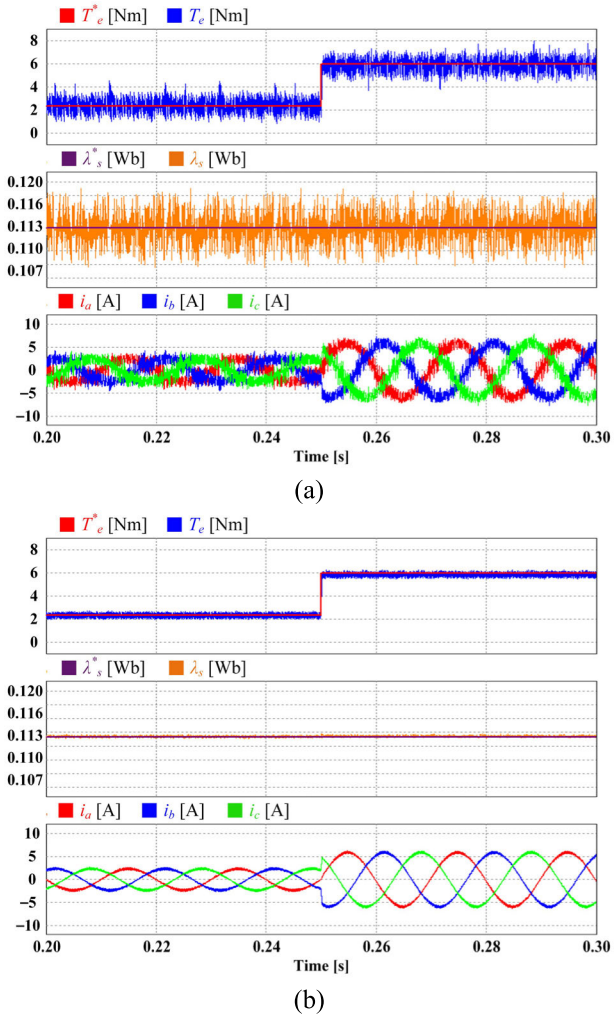

FIGURE 7. Simulation results of torque control at 500 rpm. (a) CMPC method and (b) proposed MPC-SVM method.

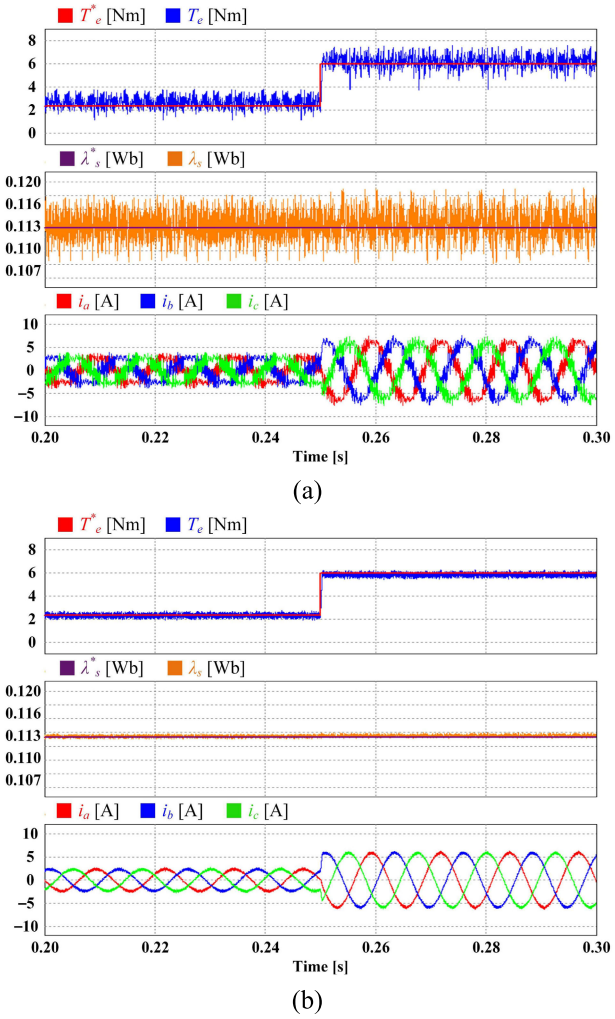

FIGURE 8. Simulation results of torque control at 800 rpm. (a) CMPC method and (b) proposed MPC-SVM method.

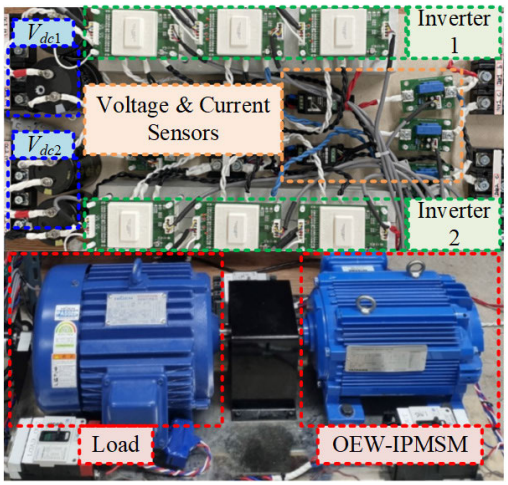

FIGURE 9. Experimental setup for the proposed method.

proposed MPC-SVM method. In the same manner as described for Fig. 10, the reference electrical torque was changed from 2.4 Nm to 6 Nm. The magnitude of average electrical torque ripple compared to the reference value was decreased from 3.77 Nm to 0.89 Nm, thus resulting in an improvement in steady-state.

Fig. 11(a) and 11(b) show the experimental results of speed control and torque control in the proposed MPC-SVM method. For the high-speed region, DC-link voltages were applied at 150 V. In Fig. 11(a), the speed was changed from 900 rpm to 1500 rpm at 2.4 Nm, while in Fig. 11(b), the reference electrical torque was changed from 2.4 Nm to 6 Nm at 1300 rpm. The proposed method was confirmed to lead to an improvement in the high-speed operation, which was hindered by the high ripple in the CMPC method.

Fig 13(a) and 13(b) show the experimental results of FFT of *b*-phase current and the minimum value of the cost function in the proposed MPC-SVM method compared to the CMPC method. The speed was 500 rpm and the electrical torque was 6 Nm. The minimum value of the cost function was decreased and the magnitude of i_b was decreased in harmonic frequency. The maximum magnitude of FFT was improved

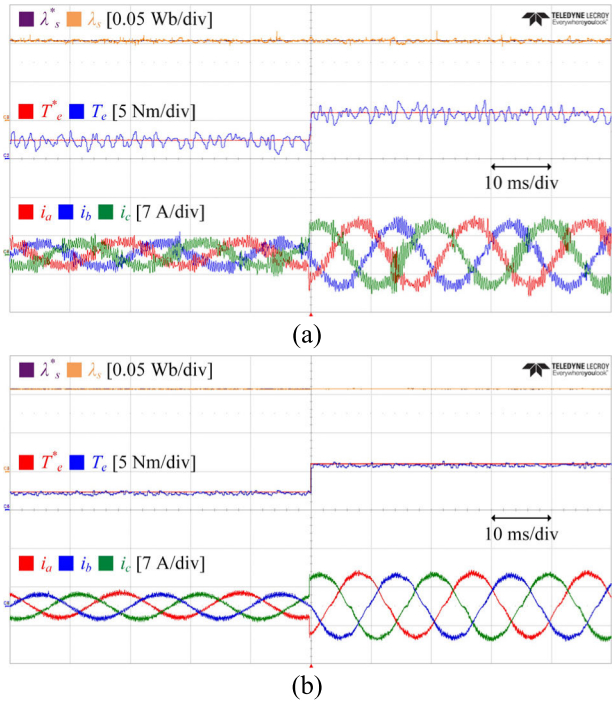

FIGURE 10. Experimental results of torque control at 500 rpm. (a) CMPC method and (b) proposed MPC-SVM method.

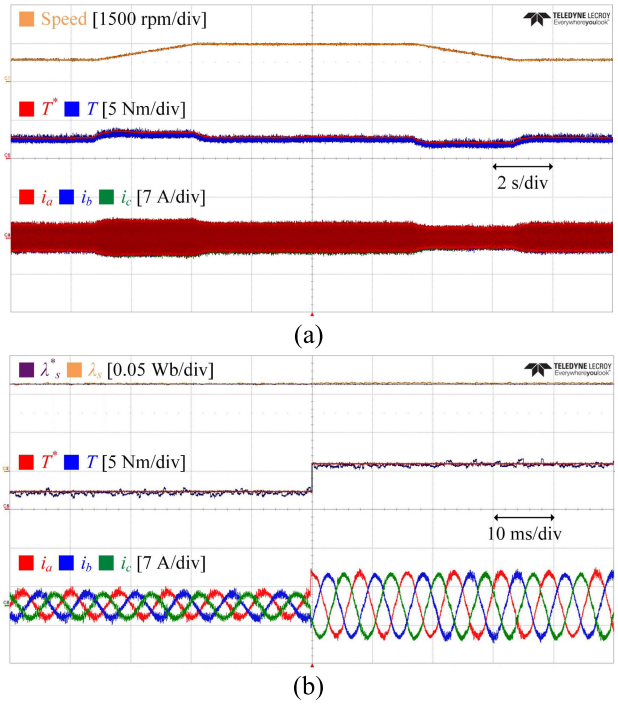

FIGURE 12. Experimental results at the high-speed region in the proposed method. (a) Speed control and (b) torque control.

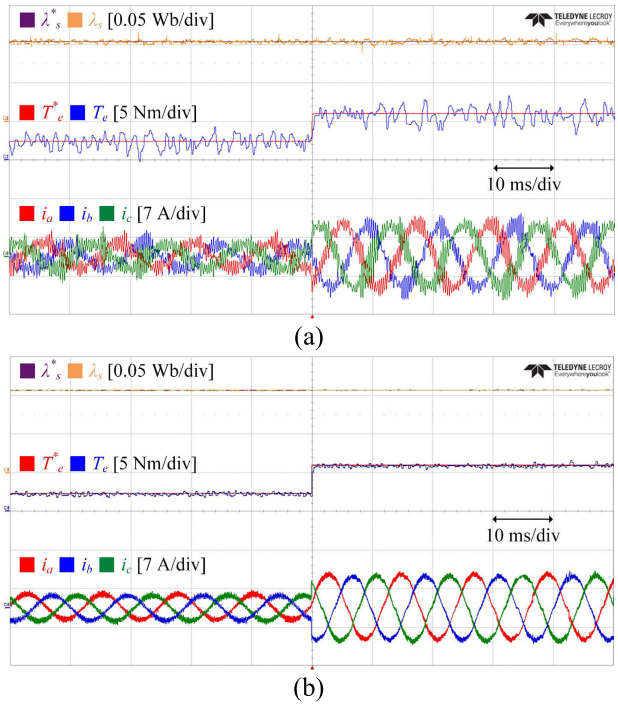

FIGURE 11. Experimental results of torque control at 800 rpm. (a) CMPC method and (b) proposed MPC-SVM method.

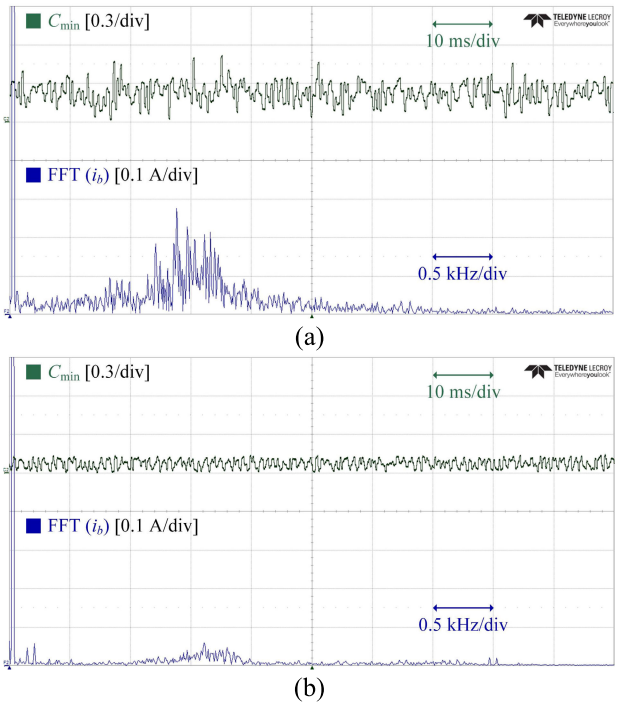

FIGURE 13. Experimental results of FFT and minimum value of the cost function. (a) CMPC method and (b) proposed MPC-SVM method.

from 280 mA to 66 mA. The average execution time for CMPC and the proposed method was 37.33 μs and 33.64 μs, respectively. Since the difference in the numbers of the candidate voltage vectors was not significant, the improvement in execution time of the proposed method was about 4 μs. However, the proposed method exhibited improved current quality compared to the CMPC from the results in Fig. 13.

VII. CONCLUSION

This paper proposed an MPC-SVM method based on a voltage angle for driving an OEW-IPMSM to improve the steady-state characteristics. In the proposed method, the voltage angle was estimated and used for the generation of virtual voltage vectors in the specific region, which is referred to as the deadbeat method. Under the lower calculation burden on the microprocessor, the ripple components of stator flux and electrical torque and THD of current were decreased compared to those in the CMPC method. Further, a more optimal voltage vector was selected in the proposed method, as the magnitude of the currents in harmonic frequency and the minimum value of the cost function were decreased. Moreover, the dead time compensation method was applied to compensate for the effect of the settled dead time of switching devices. The validity of the proposed MPC-SVM method was demonstrated through the simulation and experimental results.

REFERENCES

[1] K.-B. Lee, *Advanced Power Electronics*. Seoul, South Korea: Munundang, 2019.
[2] H.-W. Lee, S.-J. Jang, and K.-B. Lee, "Advanced DPWM method for switching loss reduction in isolated DC type dual inverter with open-end winding IPMSM," *IEEE Access*, vol. 11, pp. 2700–2710, 2023.
[3] Y. Lee and J.-I. Ha, "Hybrid modulation of dual inverter for open-end permanent magnet synchronous motor," *IEEE Trans. Power Electron.*, vol. 30, no. 6, pp. 3286–3299, Jun. 2015.
[4] Q. An, J. Liu, Z. Peng, L. Sun, and L. Sun, "Dual-space vector control of open-end winding permanent magnet synchronous motor drive fed by dual inverter," *IEEE Trans. Power Electron.*, vol. 31, no. 12, pp. 8329–8342, Dec. 2016.
[5] P. Sandulescu, F. Meinguet, X. Kestelyn, E. Semail, and A. Bruyère, "Control strategies for open-end winding drives operating in the flux-weakening region," *IEEE Trans. Power Electron.*, vol. 29, no. 9, pp. 4829–4842, Sep. 2014.
[6] P. Naganathan and S. Srinivas, "Voltage-injected PWM variants for a dual two-level inverter-fed open-end winding induction motor drive," *IEEE J. Emerg. Sel. Topics Power Electron.*, vol. 9, no. 2, pp. 1532–1540, Apr. 2021.
[7] W. Zhao, P. Zhao, D. Xu, Z. Chen, and J. Zhu, "Hybrid modulation fault-tolerant control of open-end windings linear Vernier permanent-magnet motor with floating capacitor inverter," *IEEE Trans. Power Electron.*, vol. 34, no. 3, pp. 2563–2572, Mar. 2019.
[8] P. Cortés, M. P. Kazmierkowski, R. M. Kennel, D. E. Quevedo, and J. Rodríguez, "Predictive control in power electronics and drives," *IEEE Trans. Ind. Electron.*, vol. 55, no. 12, pp. 4312–4324, Oct. 2008.
[9] F. Niu, B. Wang, A. S. Babel, K. Li, and E. G. Strangas, "Comparative evaluation of direct torque control strategies for permanent magnet synchronous machines," *IEEE Trans. Power Electron.*, vol. 31, no. 2, pp. 1408–1424, Feb. 2016.
[10] J.-S. Lee, K.-B. Lee, and F. Blaabjerg, "Predictive control with discrete space-vector modulation of Vienna rectifier for driving PMSG of wind turbine systems," *IEEE Trans. Power Electron.*, vol. 34, no. 12, pp. 12368–12383, Dec. 2019.
[11] S. Kouro, P. Cortes, R. Vergas, U. Ammann, and J. Rodriguez, "Model predictive control—A simple and powerful method to control power converters," *IEEE Trans. Ind. Electron.*, vol. 56, no. 6, pp. 1826–1838, Jun. 2009.
[12] J. Gao, C. Gong, W. Li, and J. Liu, "Novel compensation strategy for calculation delay of finite control set model predictive current control in PMSM," *IEEE Trans. Ind. Electron.*, vol. 67, no. 7, pp. 5816–5819, Jul. 2020.
[13] X. Zhang, G. H. B. Foo, T. Jiao, T. Ngo, and C. H. T. Lee, "A simplified deadbeat based predictive torque control for three-level simplified neutral point clamped inverter fed IPMSM drives using SVM," *IEEE Trans. Energy Convers.*, vol. 34, no. 4, pp. 1906–1916, Dec. 2019.
[14] F. Morel, X. Lin-Shi, J.-M. Retif, B. Allard, and C. Buttay, "A comparative study of predictive current control schemes for a permanent-magnet synchronous machine drive," *IEEE Trans. Ind. Electron.*, vol. 56, no. 7, pp. 2715–2728, Jul. 2009.
[15] A. Andersson and T. Thiringer, "Assessment of an improved finite control set model predictive current controller for automotive propulsion applications," *IEEE Trans. Ind. Electron.*, vol. 67, no. 1, pp. 91–100, Jan. 2020.
[16] I. M. Alsofyani and K.-B. Lee, "A unidirectional voltage vector preselection strategy for optimizing model predictive torque control with discrete space vector modulation of IPMSM," *IEEE Trans. Ind. Electron.*, vol. 69, no. 12, pp. 12305–12315, Dec. 2022.
[17] H. Wang, X. Wu, X. Zheng, and X. Yuan, "Virtual voltage vector based model predictive control for a nine-phase open-end winding PMSM with a common DC bus," *IEEE Trans. Ind. Electron.*, vol. 69, no. 6, pp. 5386–5397, Jun. 2022.
[18] Y. Wang, X. Wang, W. Xie, F. Wang, M. Dou, R. M. Kennel, R. D. Lorenz, and D. Gerling, "Deadbeat model-predictive torque control with discrete space-vector modulation for PMSM drives," *IEEE Trans. Ind. Electron.*, vol. 64, no. 5, pp. 3537–3547, May 2017.
[19] J.-H. Lee, J.-S. Lee, H.-C. Moon, and K.-B. Lee, "An improved finite-set model predictive control based on discrete space vector modulation methods for grid-connected three-level voltage source inverter," *IEEE J. Emerg. Sel. Topics Power Electron.*, vol. 6, no. 4, pp. 1744–1760, Dec. 2018.
[20] D.-H. Lee and J.-W. Ahn, "A simple and direct dead-time effect compensation scheme in PWM-VSI," *IEEE Trans. Ind. Appl.*, vol. 50, no. 5, pp. 3017–3025, Sep. 2014.

HYUNG-WOO LEE (Student Member, IEEE) received the B.S. and M.S. degrees in electrical and computer engineering from Ajou University, Suwon-si, South Korea, in 2020 and 2022, respectively, where he is currently pursuing the Ph.D. degree in electrical and computer engineering. His research interests include dual inverters, electric machine drives, and power conversion.

TAE-YONG YOON (Student Member, IEEE) received the B.S. and M.S. degrees in electrical and computer engineering from Ajou University, Suwon-si, South Korea, in 2022 and 2024, respectively. Since 2024, he has been with Samsung Electronics, Suwon-si. His current research interests include electric machine drives and dual inverters.

KYO-BEUM LEE (Senior Member, IEEE) received the B.S. and M.S. degrees in electrical and electronic engineering from Ajou University, Suwon-si, South Korea, in 1997 and 1999, respectively, and the Ph.D. degree in electrical engineering from Korea University, Seoul, South Korea, in 2003.

From 2003 to 2006, he was with the Institute of Energy Technology, Aalborg University, Aalborg, Denmark. From 2006 to 2007, he was with the Division of Electronics and Information Engineering, Jeonbuk National University, Jeonju-si, South Korea. In 2007, he joined the Department of Electrical and Computer Engineering, Ajou University. His research interests include electric machine drives, renewable power generation, and electric vehicle applications. He is currently the Editor-in-Chief of *Journal of Power Electronics*. He is an Associate Editor of IEEE TRANSACTIONS ON POWER ELECTRONICS.